COBEM 2023
27TH INTERNATIONAL CONGRESS OF MECHANICAL ENGENEERING

ABCM Brazilian Society of Mechanical Sciences and Engineering
27th ABCM International Congress of Mechanical Engineering
December 04-08, 2023, Florianópolis-SC, Brazil

COB-2023-0405
TRANSIENT MODEL FOR THE INTERNAL PRESSURE OF VACUUM INSULATION PANELS

Mateus Henrique Corrêa
Cristiano Bigonha Tibiriçá
Heat Transfer Research Group, Department of Mechanical Engineering, Escola de Engenharia de São Carlos (EESC), University of São Paulo (USP), Av. Trabalhador São-carlense, 400, 13566-970 São Carlos, SP, Brazil
mateus.hcorrea@usp.br
bigonha@sc.usp.br

Abstract. *Vacuum Insulation Panels (VIP) are a technology of high-performance insulators that consists of a core material at low pressure, usually powders or fibers, and an envelope to protect the core from the outside gases. In order to better model a VIP thermal performance, the core pressure variation along time should be well predicted, including effects of mass transfer, leakage and residual gases trapped inside the panels. In this context, a transient model for the internal pressure was developed and used to compare against experimental data. That model consists on a two control volumes, the internal volume (volume of the measurement system plus the available gas volume of the core) and the trapped gas volume. An experimental setup consisting of a VIP of 200x200x10 cubic millimeters was used for tests. The predicted internal pressure 66 thousand seconds after the beginning of the experiment in comparison with the collected data has shown an error of less than 4%, indicating that the envelope has great effect on the internal pressure. The effective thermal conductivity of* $5.5 \cdot 10^{-3}$ *W/mK was achieved using an appropriated envelope to maintain the core pressure as low as necessary for the tests for a hot side with heat load of 8.1 W, approximately.*

Keywords: *Vacuum Insulation Panel, transient internal pressure model, thermal conductivity.*

1. INTRODUCTION

VIPs are insulators gaining space on industry and building applications due to its low thermal conductivity. It is composed by a core material at very low pressure covered by an envelope to protect against outside gases. Figure 1 shows the structure of most manufactured VIPs.

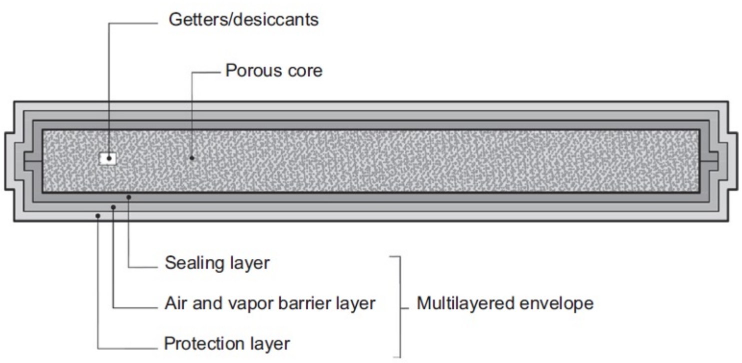

Figure 1. Structure of a vacuum insulating panel. Source: Casini (2016)

As can be seen, a barrier to air and vapour is very important to maintain the low pressure inside, and the materials of this layer must be carefully selected. Visco *et al.* (2021) has shown that polyethylene-based films, used as sealant materials, have a diffusivity of gases through it as function of the temperature, and at the range of operating temperature of a VIP, this materials are not as sealant as necessary.

So, a aluminium layer could be a solution for air and vapour barrier. However, as a manufactured defect, pinholes are present in these layers (Dai *et al.*, 2014), making it a not good enough barrier to the air. Thus, a combination of Al-layer and polymers layers are a very effective envelope for a VIP, because the molecules have a more difficult path to the interior.

As can be seen in Fig. 2, the performance of a VIP is a function of the internal pressure, and every core material has a different behavior.

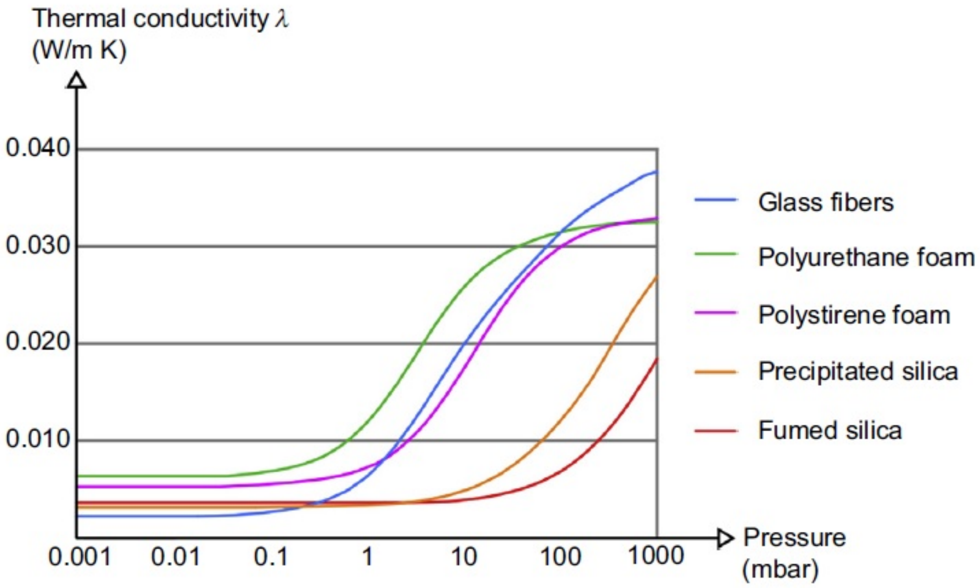

Figure 2. Thermal conductivity of vacuum insulating panels related to operating pressure and core material. Source: Casini (2016)

As the diffusion of gases through the envelope is inevitable, and the thermal conductivity is a function of the internal pressure, the selection of the adequate core material, as well as a model for the internal pressure, are determinant for the life-time prediction.

For this present study, fumed silica was chosen as core material, mainly because its gaseous conductivity (and so the effective thermal conductivity) is less effected with increasing pressure when compared to other materials as well as its performance is better than these others at atmospheric pressure.

2. METHODOLOGY

In this section the experimental apparatus will be discussed in detail as well as the models for the internal pressure and the thermal conductivity of the VIP. For the setup, it is presented the assembly, tested conditions and uncertainties, and for the models, all necessary equations are listed.

2.1 Experimental apparatus

For the experimental setup, the Joule effect was used to product heat in one side of the VIP, so, a base composed by a resistance and a 200x200 mm aluminium plate (used to uniformed the temperature) - insulated at the bottom and at the sides - was built to perform the hot surface.

To provide direct current to the base, the power supply used was a Minipa MPC-3006D, and to monitor the voltage and the current, a high impedance voltage divider and a ACS712ELC-20A sensor was used, respectively.

To pump the air out of the system, a SURYHA 12 CFM vacuum pump with a filter - to protect against residual powder - was used, and the pressure was measured by a MPXV6115V sensor. Figure 3 shows the apparatus .

All tubes are made of copper with brass connections and o-rings, to minimize mass diffusion and leakages. Figure 4 shows the schematic of these connections and main components for the vacuum.

The temperatures of the base (T_b), the top of the VIP (T_t) and the ambient air (T_{amb}) were measured by 3 NTC 10 kΩ, as can be seen in Fig. 5. All readings were collected by an USB-6001 NI.

The VIP itself consists in a 200x200x10 mm ABS 3D printed base with 0.5 mm thickness used as armature for the silica, and covered by paper both sides (bottom and top), as can be seen in Fig. 6.

2.2 Tested conditions and uncertainties

There were made two battery tests, the pressure model validation, in which there was not heat transfer, and the thermal conductivity model validation.

On the first one, a 12 μm Nylon®-polyethylene film was used as envelope, because its diffusivity was high enough to permit the increase of pressure be notice along days.

And on the second, a laminated aluminium-LDPE-polyethylene foil 200μm was used as envelope and the VIP was

Figure 3. Experimental apparatus. Source: author.

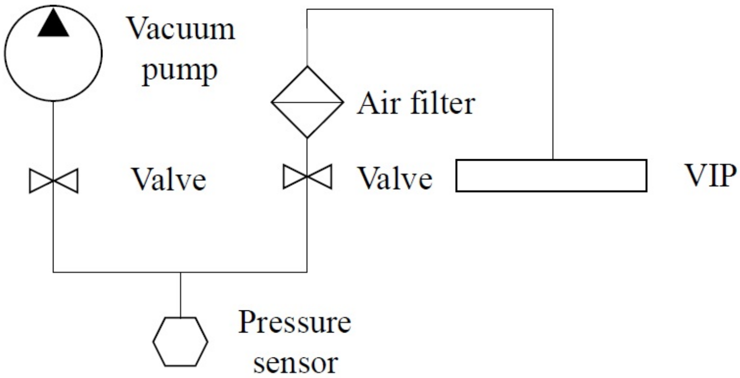

Figure 4. Schematic of the connections. Source: author.

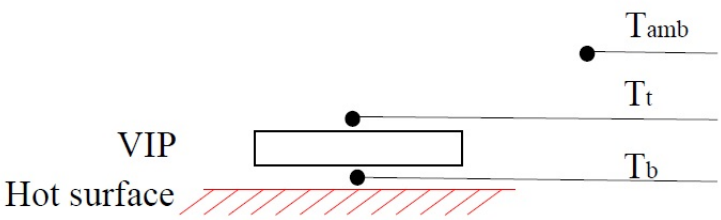

Figure 5. Schematic of the temperature sensors. Source: author.

submitted at a hot surface. The voltage applied on the terminal of the base was 8.1 V and the current was 1.0 A, totaling 8.1 W, approximately. All uncertainties are listed in Tab. 1.

2.3 Models for VIP

In this subsection, the internal pressure model will be scrutinized. This model contemplates all relevant contributions for the increase of pressure. Also, the thermal conductivity model as function of the internal pressure for the fumed silica is presented.

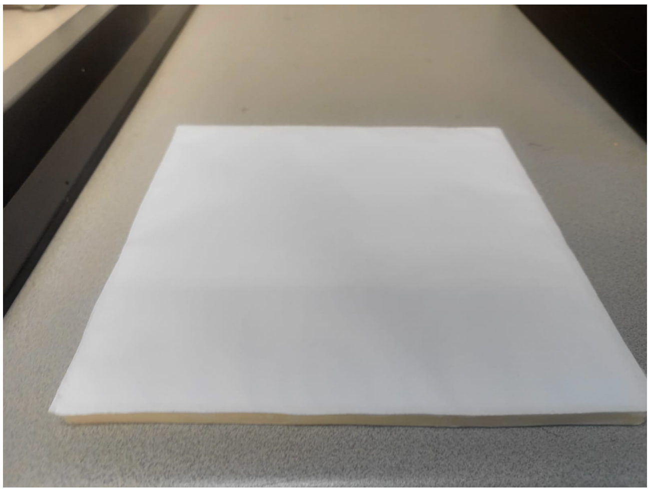

Figure 6. VIP. Source: author.

Table 1. Uncertainties. Source: author.

Measure	Uncertainty
Pressure (Pa)	20
Temperatures (K)	0.3
Lenght (mm)	0.1
Voltage (V)	0.01
Current (A)	0.01

2.3.1 Pressure model

For the pressure model, there are three important phenomenons to notice, the leakages of the measurement system, the mass diffusion through the envelope and the gas trapped in the silica powder diffusing to the whole system at low flow rate.

The first one is described by a Darcy Law, and its proportionality constant is acquired experimentally.

$$\frac{dm_1}{dt} = n \cdot dP^{1/2} \tag{1}$$

where dm_1/dt is the leakage flow rate, n is a proportionality constant and dP is the pressure difference between internal and external pressure (atmosphere). Integrating it in time,

$$m_1(t) = n \int_0^t [P_{ext} - P(t)]^{1/2} \tag{2}$$

where P_ext is the external pressure and P(t) is the internal pressure measured by the sensor.

The second one, the mass diffusion, is modelled by Fick's Law.

$$\frac{dm_2}{dt} = D \cdot A \cdot \frac{dC}{dx} \tag{3}$$

where dm_2/dt is the mass flow rate by the diffusion, D is the diffusivity, A is the diffusivity area and dC/dx is the concentration difference along thichness. dC can be described as:

$$dC = \rho_{atm} - \frac{m(t)}{V} \tag{4}$$

where ρ_{atm} is the density of the atmosphere, m(t) is the internal mass of gases and V is the total internal volume, which can be represented as:

$$V = A_{VIP} \cdot w \cdot \epsilon + V_{ms} \tag{5}$$

where A_{VIP} is the area of the VIP, w is its width, ϵ is its porosity and V_{ms} is the volume of the measurement system.

According to Mehrer (2007), the diffusion coefficient D can be expressed as function of the temperature, as shown in Eq. 6.

$$D = D_0 \cdot e^{\frac{\Delta E}{kT}} \tag{6}$$

where D_0 is the maximum diffusivity, k is the Boltzmann constant, T is the temperature in Kelvin and ΔE is the activation energy, which can be obtained by measuring the diffusivity at two different temperatures:

$$\Delta E = \frac{k \cdot ln(\frac{D_1}{D_2})}{\frac{1}{T_2} - \frac{1}{T_1}} \tag{7}$$

where D_1 and D_2 are the diffusivities measured at T_1 and T_2, respectively.

For the last one, the gas trapped inside, it was assumed a second control volume (smaller than the total internal volume) connected to the the hole system. So, the mass flow rate between these two control volumes can be expressed by Darcy's Law, similarly to Eq. 1.

$$\frac{dm_3}{dt} = b \int_0^t [P_t(t) - P(t)]^{1/2} \tag{8}$$

where dm_3/dt is the mass flow rate of the gas trapped to the whole system, b is the proportionality constant (experimental) and $P_t(t)$ is the pressure of the gas trapped.

So, having these equations, the internal gas mass can be expressed as the sum of all partial contributions.

$$m(t) = \sum_{i=1}^{3} m_i \tag{9}$$

This way, the internal pressure of the VIP can be obtained by Eq. 10.

$$P_{VIP} = m(t) \cdot \frac{R \cdot T}{V} \tag{10}$$

where T is the temperature of the gas on the VIP.

2.3.2 Thermal conductivity model

The thermal conductivity of a core of a VIP can be expressed in three parts, solid, gaseous and radioactive thermal conductivity. The first one, the solid, is given by Eq. 11 (Kaganer, 1969).

$$k_s = 3.4 \cdot k_p \cdot (1 - \Pi)^{1/2} \cdot (P_{atm} \frac{1 - \nu^2}{E})^{1/3} \tag{11}$$

where k_s is the effective thermal conductivity, k_p is the thermal conductivity of a fumed silica particle, Π is the porosity, P_{atm} is the atmospheric pressure, ν is the Poisson's ratio and E is the Young's modulus of elasticity for fumed silica.

The second, gaseous, is given by Eq. 12 (Kwon *et al.*, 2009).

$$k_g = \frac{k_0}{(1 + 0.032/P\phi)} \tag{12}$$

where k_0 is the gaseous conductivity of free still air at 300K, P the gas internal pressure and ϕ the pore size.

the third, radioactive, can be simply calculated by using Eq. 13 (Caps *et al.*, 1983).

$$k_r = \frac{16 \cdot n^2 \cdot \sigma \cdot T^3}{3 \cdot E(T)} \tag{13}$$

where n is the refractive index, σ is the Stefan–Boltzmann constant, T is the mean temperature and E(T) is the Rosseland mean extinction coefficient.

This way, the thermal conductivity of the core material (fumed silica) of the VIP can be obtained by the sum of each part, as shown in Eq. 14

$$k_{core,total} = k_s + k_g + k_r \tag{14}$$

2.4 Data reduction

In this subsection, the collected data by the tests will be converted to the thermal conductivity by using two different methods. The first, by using the thermal resistance to the ambient, the heat lost for the ambient is measured, and the second, the average local heat transfer coefficient is determined. In both methods, the same material is used to measure the necessary quantities.

2.4.1 Thermal conductivity by ambient resistance

To determine the thermal conductivity of the VIP by using thermal resistance, it is important to compute how much heat is lost to the ambient. So, a material with the same geometry of the VIP, but with a well-known thermal conductivity is used to calibrate the thermal resistance from the base to the ambient, as can be seen in Eq. 15.

$$R_{amb} = w_m \cdot \frac{T_b - T_{amb}}{U \cdot I \cdot w - k_m \cdot A \cdot (T_b - T_t)} \tag{15}$$

where R_{amb} is the thermal resistance from the base to the ambient, U is the voltage, I is the current, k_m is the thermal conductivity of the material, w_m is the width of the material and A is the area.

With the thermal load applied - monitored by the voltage and current sensors - and the heat losses to the ambient, computed through R_{amb}, it is possible to determine the thermal conductivity of the VIP, as shown in Eq. 16.

$$k_{VIP-R} = \frac{R_{amb} \cdot U \cdot I \cdot w - (T_b - T_{amb}) \cdot w}{R_{amb} \cdot A \cdot (T_b - T_t)} \tag{16}$$

where k_{VIP-R} is the thermal conductivity of the VIP by ambient resistance and w is the width of the VIP.

2.4.2 Thermal conductivity by natural convection

To determine the thermal conductivity of the VIP by natural convection, a material with a well-known thermal conductivity was used to measure an average local heat transfer coefficient. With this coefficient it is possible to determine the thermal conductivity of the VIP, as shown in Eq. 17.

$$k_{VIP-NC} = h \cdot w \cdot \frac{(T_t - T_{amb})}{(T_b - T_t)} \tag{17}$$

where k_{VIP-NC} is the thermal conductivity of the VIP by average local heat transfer coefficient and h can be expressed as:

$$h = \frac{k_m \cdot (T_b - Tt) - \varepsilon \cdot \sigma \cdot (T_t^4 - T_{amb}^4)}{T_t - T_{amb}} \tag{18}$$

where ε is the emissivity of the material and σ is the Stefan-Boltzmann constant.

3. RESULTS AND DISCUSSION

In this section, the results for the pressure model as well as the thermal conductivity - by ambient resistance and by heat transfer coefficient - are presented.

3.1 Pressure Model

For the pressure model, the system of equations were solved numerically, and time step of "dt s" was used. Figure 7 shows the comparison between predicted and measured internal pressure of the VIP.

As can be seen, the model has shown a satisfactory achievement for the study of leakages, mass diffusion and trapped gas influences. The difference between the predicted and the measured pressures after 66 thousand seconds was 3.3%, approximately.

Figure 8 shows the same data, but just the first 1200 seconds of the test. It is possible to notice that the model has a much better correlation with the observed in this interval. One of the reasons is related with the pressure sensor, which do not measure the internal pressure itself, but the difference between internal and external. That is the reason for the oscillating behavior of the measured pressure the variation of atmospheric pressure in Fig. 7.

To compute this variation, it was used the available data of a local weather station. The pressure were actualized hour by hour, and all pressures between one hour and other was approximated by using a 3þdegree polynomial.

Even with this limitation with the measured pressure, it was notable that this model has shown that the leakages of the measurement system and the mass diffusion through the film was to important to be negligible to the tests. After

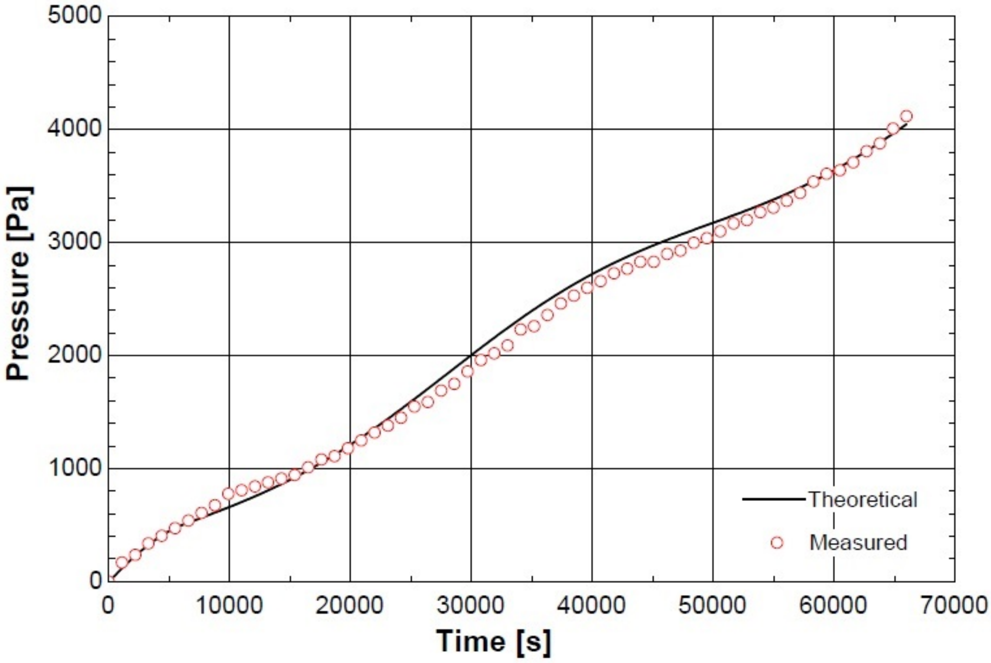

Figure 7. Comparison between predicted and measured internal pressure for a 12μm film. Source: author.

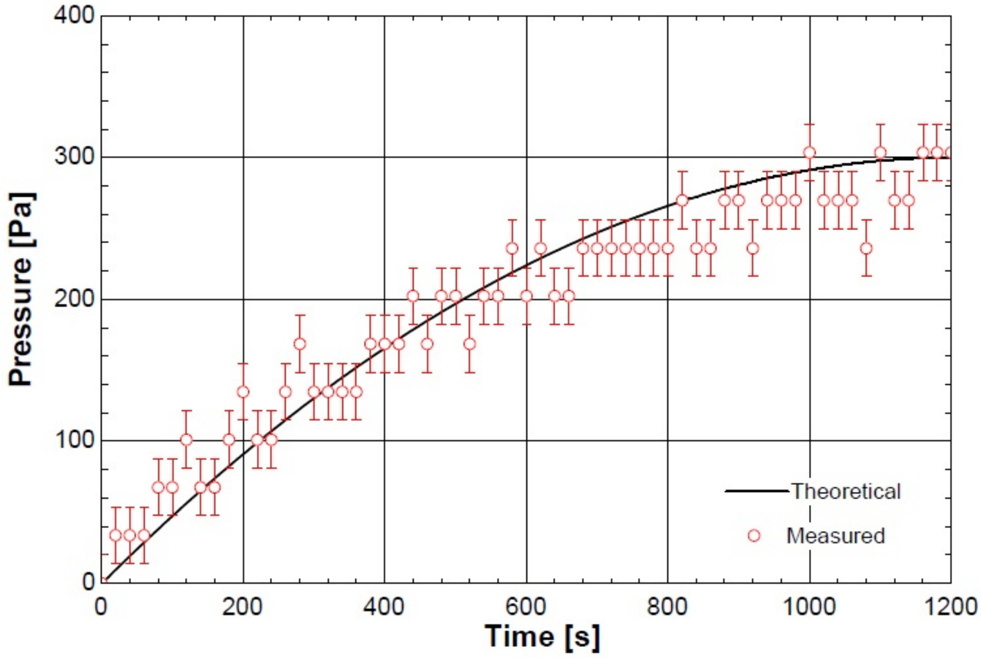

Figure 8. Comparison between predicted and measured internal pressure for a 12μm film. Source: author.

verifying these problems, the measurement connections were re-designed and the film was substituted by an aluminium foil envelope. Figure 9 shows the predicted and measured pressures after these modifications.

It is possible to notice the difference between before (Fig. 7) and after (Fig. 9) the modifications. With these modifications, it was observed an increase of pressure of almost 50 Pa in 63 thousand seconds, which is stable enough to measure the thermal conductivity of the VIP at different levels of pressure.

3.2 Thermal conductivity

With the pressure model validated and the increasing of pressure at satisfactory rate, it was possible to determine the effective thermal conductivity of the VIP and compare against the predicted, as can be seen in Fig. 10, by using the

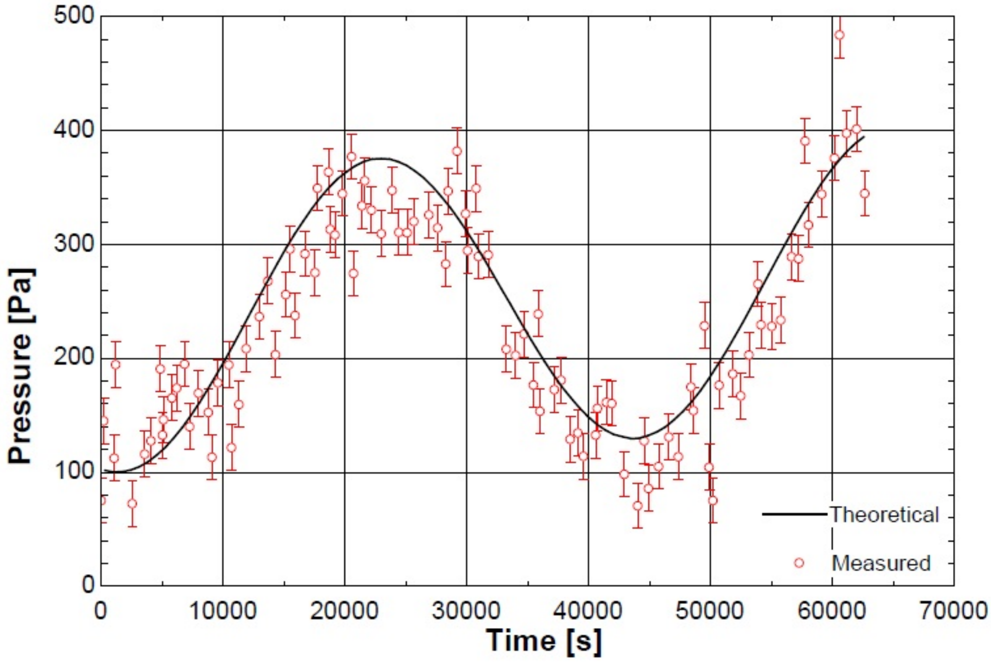

Figure 9. Comparison between predicted and measured internal pressure after modifications. Source: author.

average local heat transfer coefficient, and Fig. 11 by using thermal resistance to the ambient.

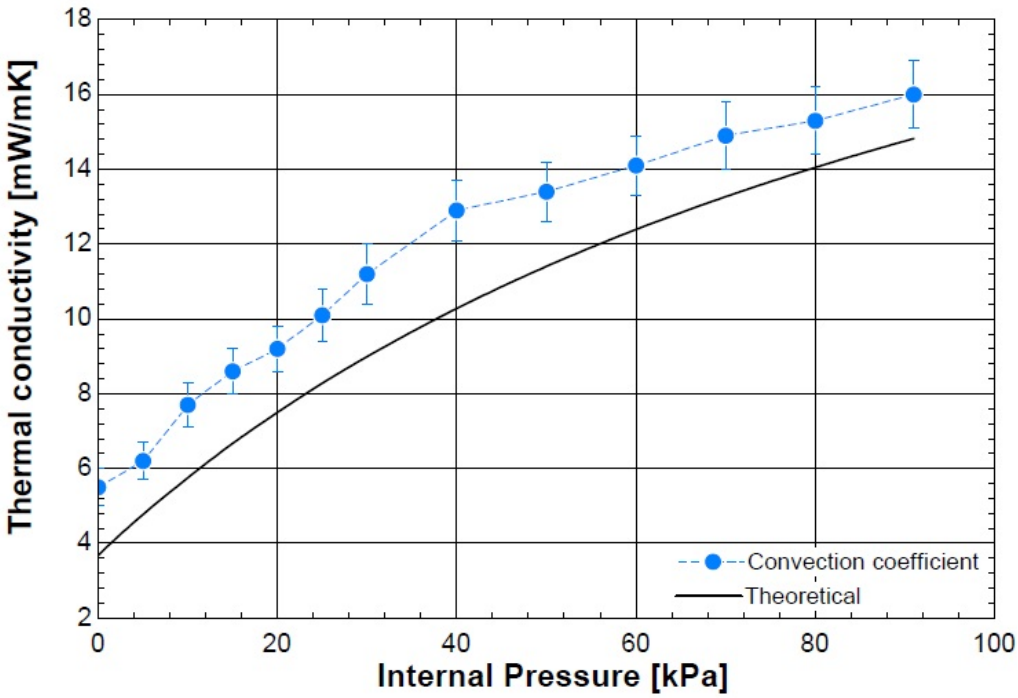

Figure 10. Effective thermal conductivity as function of internal pressure by average heat transfer coefficient. Source: author.

It is notable the difference between these two methods to obtain the effective thermal conductivity of the VIP. The uncertainties for the heat transfer coefficient method are smaller than the thermal resistance method, however, it is possible to notice that both methods are close to a common tendency of increasing thermal conductivity with pressure. Fig 12 shows the comparison between predicted model and collect data by average heat transfer coefficient. The limits are 30%.

From this comparison it is possible to see that the model has under-predicted the behavior of the VIP. However, it is important to notice that there is a possible non-negligible thermal bridge effect on this experiment. This effect will be studied to analyse the effective thermal performance for every VIP size.

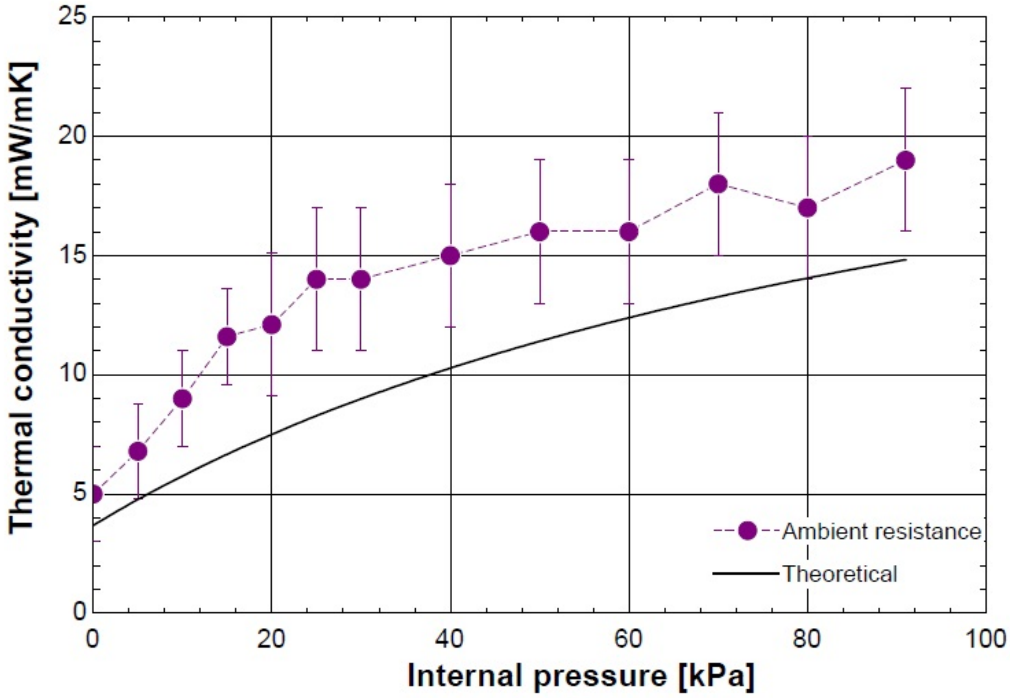

Figure 11. Effective thermal conductivity as function of internal pressure by thermal resistance to the ambient. Source: author.

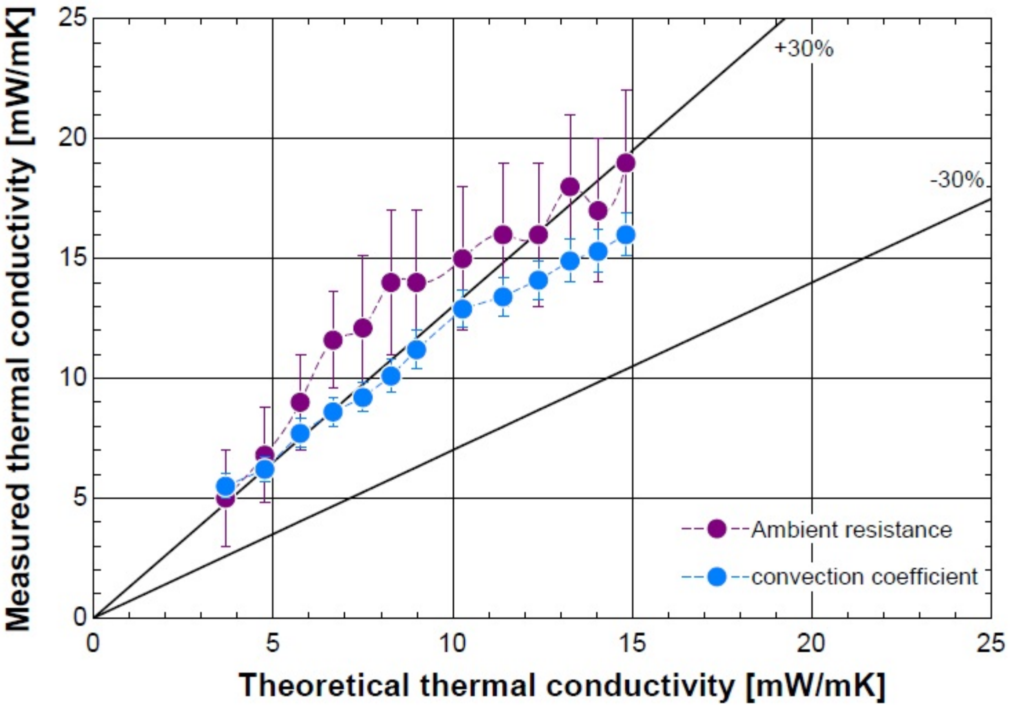

Figure 12. Comparison between predicted and measured thermal resistance of the VIP by using the average local heat transfer coefficient. Source: author.

4. CONCLUSION

For this present study, it was notable that the envelope is determinant for the working-life of the VIP as well as the size of the VIP, due to the increasing of pressure through mass diffusion and thermal bridge effect, respectively.

It was proved that metalized films, such as Al-foils, are necessary to mitigate the mass diffusion. As a result, the increasing of pressure along 63 thousand seconds was 50 Pa, approximately.

It was also tested and discovered that the best way between the two methods to obtain the thermal conductivity is by using the average local heat transfer coefficient. As a result, the lower thermal conductivity of the VIP found was $5.5 \cdot 10^{-3}$ W/mK.

For next studies, the thermal bridge effect has to be studied to determine a satisfactory size for the VIP best performance, as well as better combination of materials for the envelope and the armature.

5. ACKNOWLEDGEMENTS

The authors are grateful to Mr. Jorge N. dos Santos for providing instrumentation assembly and coding, and to the University of São Paulo for the financial support.

6. REFERENCES

Caps, R., Fricke, J. and Reiss, H., 1983. "Improving the extinction properties of an evacuated high-temperature powder insulation". *High temperature - high pressure*, Vol. 15, pp. 225–232.

Casini, M., 2016. "4 - advanced insulating materials". In M. Casini, ed., *Smart Buildings*, Woodhead Publishing, pp. 127–177. ISBN 978-0-08-100972-7. doi:https://doi.org/10.1016/B978-0-08-100635-1.00004-6.

Dai, Q., Zhang, D., Chen, X., Dong, J. and Pan, F.S., 2014. "Research on pinholes in aluminum foil". *Advanced Materials Research*, Vol. 884-885, pp. 308–311. doi:10.4028/www.scientific.net/AMR.884-885.308.

Kaganer, M.G., 1969. *Thermal insulation in cryogenic engineering*. Israel Program for Scientific Translations, Jerusalem.

Kwon, J.S., Jang, C.H., Jung, H. and Song, T.H., 2009. "Effective thermal conductivity of various filling materials for vacuum insulation panels". *International Journal of Heat and Mass Transfer*, Vol. 52, No. 23, pp. 5525–5532. doi:https://doi.org/10.1016/j.ijheatmasstransfer.2009.06.029.

Mehrer, H., 2007. *Diffusion in Solids: Fundamentals, Methods, Materials, Diffusion-Controlled Process*. Springer, New York.

Visco, A., Scolaro, C., Torrisi, A. and Torrisi, L., 2021. "Diffusion of nitrogen gas through polyethylene based films". *POLYMER CRYSTALLIZATION*, Vol. 4. doi:10.1002/pcr2.10207.

7. RESPONSIBILITY NOTICE

The authors are solely responsible for the printed material included in this paper.